Asymptotic freedom in the lattice Boltzmann theory

S. A. Hosseini and I. V. Karlin*

Department of Mechanical and Process Engineering, ETH Zurich, 8092 Zurich, Switzerland

(Received 8 August 2023; accepted 10 June 2024; published 15 July 2024)

Asymptotic freedom is a feature of quantum chromodynamics that guarantees its well posedness. We derive an analog of asymptotic freedom enabling unconditional linear stability of lattice Boltzmann simulation of hydrodynamics. We further demonstrate the validity of the derived conditions via the special case of the equilibrium based on entropy maximization, which is shown to be uniquely renormalizable.

DOI: 10.1103/PhysRevE.110.015306

I. INTRODUCTION

The lattice Boltzmann method (LBM) has become a popular tool for the simulation of complex fluid dynamics, with applications ranging from turbulent flows to multiphase [1] and multicomponent flows, combustion [2], and relativistic flows [3,4]. In LBM, a simple kinetic equation of the Boltzmann type for the populations of a controlled number of designer particles' velocities, forming links of a regular spatial lattice, is solved numerically in a "stream-along-links and relax-to-equilibrium at the nodes" fashion. Efficiency and universality are keywords that one associates with LBM.

At the same time, theoretical foundations of LBM remain obscure in lieu of longstanding issues of stability and accuracy. The issue of stability dominated LBM research ever since the appearance of the LBM in the early 1990s [5], up until very recently. The topic becomes even more intriguing upon more detailed analysis of the algorithm: The streaming step can readily be shown to be unconditionally linear stable, which means the collision step is responsible for the restricted stability domain. A variety of approaches such as the multiple relaxation class of models [6,7] has been developed in the literature, each leading to an incremental increase in stability domain, and all coming at the cost of considerable hyperviscosity. Furthermore, none of the proposed extensions on the LBM have allowed it to operate beyond the limit,

$$|u|^{\max} = 1 - \frac{1}{\sqrt{3}} \approx 0.42; \tag{1}$$

see [8–10]. Considering that the collisionless system of partial differential equations is stable, it is, again, clear that the collision operator is the root of the instabilities. In deriving the proper collision operator, two ingredients can be modified: (a) the attractor or equilibrium state and (b) the relaxation path. While the latter has been the ingredient of choice for most schemes, it is clear that it cannot be a *necessary* or *sufficient* condition for stability. A necessary condition for stability of the relaxation from a given state to the attractor, in other words, a convex combination of both states, would be that both are stable [11].

In a previous publication (see [10]), a detailed and meticulous study showed that the entropic LBM and corresponding discrete equilibrium attractor are the only candidates in the literature satisfying the above-mentioned condition on stability of the attractor over $u \in [-1, 1]$. Building upon experience gained from the analysis of the entropic equilibrium, in this paper, we propose a different approach to LBM by following the ideas of renormalization group [12–14]. We derive the necessary and sufficient conditions of linear stability with a focus on the one-dimensional (1D) D1Q3 system, as conditions for linear stability of the 1D system are necessary for any higher-dimensional realization. We find that unconditional stability implies vanishing pressure at large flow velocity, which bears direct analogy to asymptotic freedom in quantum chromodynamics [15–17]. We show that this change of paradigm in deriving equilibria leads to unconditionally stable lattice Boltzmann models.

II. GENERIC LBGK

We consider the lattice Bhatnagar-Gross-Krook (LBGK) model [18] for nearly incompressible flows,

$$f_i(\boldsymbol{r} + \boldsymbol{c}_i\delta t, t + \delta t) - f_i(\boldsymbol{r}, t) = 2\beta\left[f_i^{\mathrm{eq}}(\rho, \boldsymbol{u}) - f_i\right]. \tag{2}$$

Here, f_i are the populations of the discrete velocities $\boldsymbol{c}_i$, $i = 1, \ldots, Q$, $\boldsymbol{r}$ is the position in space, t is the time, δt is the time step, ρ is the fluid density, and $\boldsymbol{u}$ is the flow velocity,

$$\sum_{i=1}^{Q} \{1, \boldsymbol{c}_i\} f_i = \{\rho, \rho\boldsymbol{u}\}. \tag{3}$$

Furthermore, $\beta \in [0, 1]$ is the relaxation parameter which is tied to the viscosity,

$$\nu = \varsigma^2 \delta t \left(\frac{1}{2\beta} - \frac{1}{2}\right), \tag{4}$$

*Contact author: ikarlin@ethz.ch

where $\varsigma = c_s \delta r/\delta t$ is the lattice speed of sound, δr is the lattice spacing, while c_s is a pure constant dependent on the choice of the lattice. Below, we use lattice units by setting $\delta r = \delta t = 1$ and consider the standard first-neighbor lattices in space dimension D defined as a D-fold tensor product of one-dimensional velocities $c_{i\alpha} \in \{-1, 0, 1\}$. These are the D$D$Q3^D lattices characterized by the lattice speed of sound,

$$\varsigma = \frac{1}{\sqrt{3}}. \tag{5}$$

A generic class of equilibria, $f_i^{\rm eq}$, is the focus of our study. First, we introduce a triplet of functions, $\Psi_{i\alpha}(\xi, \mathcal{P})$, $i\alpha \in \{-1, 0, 1\}$: $\Psi_0 = 1 - \mathcal{P}$, $\Psi_{-1} = (1/2)(-\xi + \mathcal{P})$, $\Psi_1 = (1/2)(\xi + \mathcal{P})$. For a D-dimensional lattice, equilibria are defined by a product form,

$$f_i^{\rm eq}(\rho, \boldsymbol{u}) = \rho \prod_{\alpha=1}^{D} \Psi_{i\alpha}\left(u_\alpha, \mathcal{P}^{\rm eq}_{\alpha\alpha}\right). \tag{6}$$

Here, $\mathcal{P}^{\rm eq}_{\alpha\alpha}$ are diagonal component of the equilibrium pressure tensor at unit density,

$$\mathcal{P}^{\rm eq}_{\alpha\alpha} = \pi^*_{\alpha\alpha} + u_\alpha^2. \tag{7}$$

LBGK setup becomes complete once the function $\pi^*_{\alpha\alpha}$ is specified.

At this point, a common LBM [3,4,18] suggests isotropic pressure,

$$\pi^*_{\alpha\alpha} = \varsigma^2. \tag{8}$$

While this seems natural and is equivalent to (6) matching moments of the classical Maxwellian, it should be remembered that Galilean invariance of LBM is restricted to small flow velocities, as implied by the lattice constraint, $c_{i\alpha}^3 = c_{i\alpha}$. Moreover, the second-order moment of the equilibrium is constrained as follows:

$$\frac{1}{\rho}\sum_{i=1}^{Q} c_{i\alpha}^2 f_i^{\rm eq} = \mathcal{P}^{\rm eq}_{\alpha\alpha} \leqslant 1. \tag{9}$$

Comparing (7) and (9), we conclude that the pressure has to vanish at the highest value of flow velocity,

$$\pi^*_{\alpha\alpha}|_{u_\alpha = \pm 1} = 0. \tag{10}$$

Obviously, this is not compatible with the isotropic pressure, and the question of stability of the LBM needs to be examined in view of the constraint (10).

In order to derive the pressure in a rigorous fashion, we follow a path inspired by renormalization group and define a "space of theories" by assuming that the function $\pi^*_{\alpha\alpha} \geqslant 0$, which plays a role of a coupling parameter, *may* depend on the flow velocity component u_α. Of course, admissible pressure functions shall be restricted by the consistency constraint at small flow velocity,

$$\pi^*_{\alpha\alpha} = \varsigma^2\{1 + \mathcal{O}[(u_\alpha/\varsigma)^4]\},\ u_\alpha/\varsigma \to 0, \tag{11}$$

but otherwise they are arbitrary at the outset of our analysis. Below, a coarse graining will be performed (the Chapman-Enskog calculation [19]) to identify the necessary stability conditions at the fixed point (hydrodynamic limit) and their implication for the pressure $\pi^*_{\alpha\alpha}$.

III. LINEAR STABILITY: 1D SYSTEM

A. Necessary stability condition: Vanishing lattice Knudsen number

While we conduct the analysis on the basis of the one-dimensional LBGK on the D1Q3 lattice, the outcome will be a necessary stability condition for any higher-dimensional realization. The first Chapman-Enskog approximation results in the continuity and momentum equations, $\partial_t^{(1)}\rho + \partial_x \rho u = 0$, $\partial_t^{(1)}\rho u + \partial_x \rho u^2 + \partial_x \rho \pi^* = 0$, where we omitted index x to ease notation. We perform the characteristics analysis [10], which reveals a pair of normal eigenmodes propagating with the speeds $c^\pm$,

$$c^\pm = u + \frac{1}{2}\partial_u \pi^* \pm \sqrt{\frac{1}{4}(\partial_u \pi^*)^2 + \pi^*}, \tag{12}$$

where a positive square root is assumed, $c^+ - c^- > 0$. Conversely, upon defining the two sound speeds, $\varsigma^\pm = c^\pm - u$, the pressure and its derivative are expressed as

$$\pi^* = -\varsigma^+\varsigma^-, \tag{13}$$

$$\partial_u \pi^* = \varsigma^+ + \varsigma^-. \tag{14}$$

In the second Chapman-Enskog approximation, the momentum equation is modified by a nonequilibrium term, $\partial_t^{(2)}\rho u = -\partial_x \pi^{\rm neq}$, with the nonequilibrium diagonal component of the pressure tensor as

$$\pi^{\rm neq} = -\left(\frac{1-\beta}{2\beta}\right)(2\mathcal{A}\rho\varsigma^2\partial_x u + \mathcal{B}\partial_x \rho). \tag{15}$$

Here, $\mathcal{A}$ (viscosity factor) and $\mathcal{B}$ (compressibility error) are

$$\mathcal{A} = \frac{1}{2\varsigma^2}[3\varsigma^2 - (c^+)^2 - (c^-)^2 - c^+c^-], \tag{16}$$

$$\mathcal{B} = 3\varsigma^2 u - u^3 + (c^- - u)(c^+ - u)(c^+ + c^- + u). \tag{17}$$

Finally, we perform the spectral analysis of the hydrodynamic equations, linearized around $\{\rho, u\}$, to find the following leading-order dissipation-dispersion relations for the eigenfrequencies:

$$\omega^\pm = c^\pm k + {\rm i}\nu\mathcal{R}^\pm k^2 + O(k^3), \tag{18}$$

where k is the wave vector, ${\rm i} = \sqrt{-1}$, and ν is the viscosity (4), while $\mathcal{R}^\pm$ are attenuation rates, written in terms of eigenmodes,

$$\mathcal{R}^\pm = \pm\frac{c^\pm[3\varsigma^2 - (c^\pm)^2]}{\varsigma^2(c^+ - c^-)}. \tag{19}$$

Hence, with the positivity of the viscosity ν (4) already established by the bound on the relaxation parameter $\beta \in [0, 1]$, the *necessary* stability condition of the LBGK system in the long-wave limit $k \to 0$ is the positivity of attenuation rates (19) $\mathcal{R}^\pm \geqslant 0$; see Fig. 1. The positivity domain of the viscosity factor (16) is also shown in Fig. 1.

The advantage of using eigenmodes in the present analysis is that the dissipation-dispersion relations (18) and (19) are explicit functions of $c^\pm$. The specific dependence of the attenuation rates (19) on $c^\pm$ provides for separable and independent conditions on c^+ and c^-. This allows us to immediately find

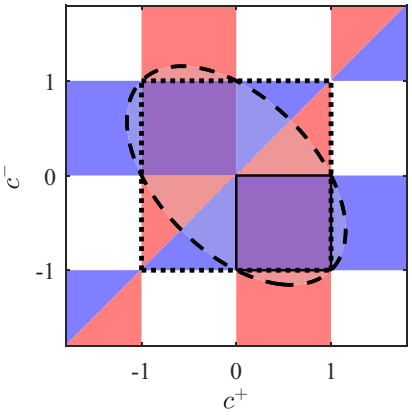

FIG. 1. Positivity domain of attenuation rates $\mathcal{R}^{\pm}$ (19) and of the viscosity factor $\mathcal{A}$ (21) as a function of eigenmodes c^+ and c^-. Red: Positivity domain of $\mathcal{R}^+$. Blue: Positivity domain of $\mathcal{R}^-$. Purple: Positivity domain of both $\mathcal{R}^+$ and $\mathcal{R}^-$ simultaneously. The positive square root convention in Eq. (12) restricts the stability domain to the bottom-right quadrant (20), shown with solid black lines. Area inside dashed black elliptic contour: Positivity domain of the viscosity factor $\mathcal{A}$ (16). Area inside dotted black square: Validity domain of CFL condition.

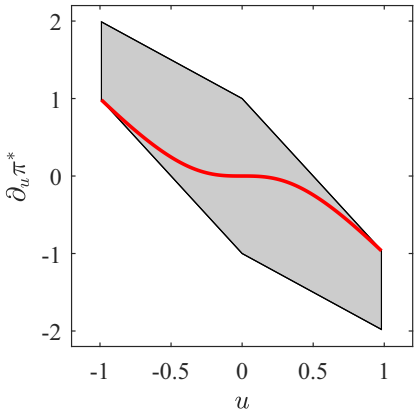

FIG. 2. Domain of existence of $\partial_u\pi^*$ under constraints of (20) and $\pi^* \geqslant 0$. Red curve shows $\partial_u\pi^*$ for the case of entropic equilibrium (28).

that attenuation rates (19) are non-negative if the eigenmodes (12) satisfy the following inequalities:

$$0 \leqslant c^+ \leqslant 1, \ -1 \leqslant c^- \leqslant 0. \tag{20}$$

Note that the *necessary stability condition* (20) is also consistent with (and is stronger than) the Courant-Friedrichs-Levy (CFL) condition [20], $\max\{|c^{\pm}|\} \leqslant 1$, which tells that no eigenmode can propagate faster than the maximal speed equal to the lattice link; see Fig. 1.

Moreover, with the explicit form of the eigenmodes (12), both the viscosity factor (16) and compressibility error (17) can equivalently be expressed in terms of the pressure π^*, its derivative $\partial_u\pi^*$, and flow velocity u,

$$\mathcal{A} = \frac{1}{2\varsigma^2}[3\varsigma^2 - 3u^2 - \pi^* - \partial_u\pi^*(3u + \partial_u\pi^*)], \tag{21}$$

$$\mathcal{B} = -(3u + \partial_u\pi^*)\pi^* + 3u\varsigma^2 - u^3. \tag{22}$$

The stability condition (20), along with non-negativity $\pi^* \geqslant 0$, implies the following limits of the pressure and its derivative at the maximal flow velocity $|u| = 1$:

$$\lim_{u\to\mp 1} \pi^* = 0, \tag{23}$$

$$1 \leqslant \lim_{u\to\mp 1} (\pm\partial_u\pi^*) \leqslant 2. \tag{24}$$

In other words, the necessary stability condition (20) for the slow modes of the D1Q3 lattice Boltzmann model implies vanishing pressure at the maximal flow velocity $|u| = 1$. The domain of existence of $\partial_u\pi^*$ under these constraints is shown in Fig. 2. Note that the additional condition on positivity of π^* restricts c^+ and c^-, as illustrated in Fig. 3.

Based on our earlier assertion of the pressure π^* as the coupling parameter, this can be interpreted as a case for *asymptotic freedom*: The necessary condition for linear stability of the lattice Boltzmann system is the asymptotic vanishing of the pressure π^* in the limit of large fluid velocity. Isotropic pressure (8) is not asymptotically free and violates the necessary stability condition (20) at $|u|^{\max}$ (1). Differently put, the pressure "needs to bend" at velocities sufficiently far from $u = 0$ and adjust in such a way as to maintain unconditional stability of the hydrodynamic limit (20). It is important to note that the conclusion drawn here on the *necessary* condition for linear stability also holds for higher-dimensional realizations since the same normal propagation modes are also present regardless of the physical dimension of the system.

B. Asymptotically free realizations

In order to find the asymptotically free pressure, we note a distinguished case when the compressibility error cancels in the nonequilibrium flux of momentum (15),

$$\mathcal{B} = 0. \tag{25}$$

With (25), the D1Q3 LBGK model becomes *renormalizable*: Since $\mathcal{A} \geqslant 0$ for the asymptotically free pressure (see Fig. 1), the viscosity factor can be absorbed into the viscosity by

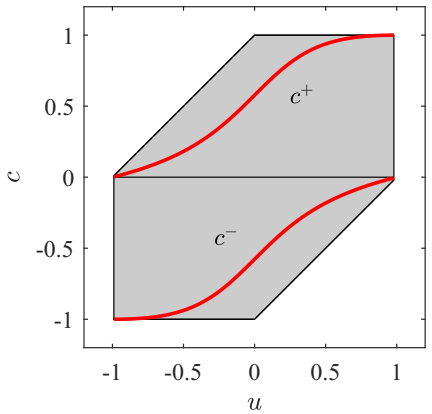

FIG. 3. Domains of existence of c^+ and c^- under constraints of (20) and $\pi^* \geqslant 0$. Red curves represent $c^{\pm}$ for the case of entropic equilibrium (28).

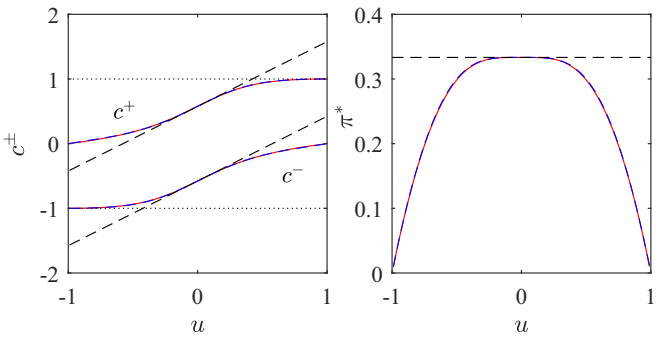

FIG. 4. Propagation speed of eigenmodes (left) and pressure π^* (right) as a function of u for Eq. (28) (red lines) and Eq. (29) (dashed blue lines). The dashed black lines represent the limit of $\pi^* = \varsigma^2$.

renormalizing the relaxation parameter,

$$\beta^* = \frac{\varsigma^2 \mathcal{A}}{2\nu + \varsigma^2 \mathcal{A}}, \tag{26}$$

whereby Eq. (15) assumes a purely Navier-Stokes form,

$$\pi^{\text{neq}} = -\frac{1-\beta^*}{2\beta^*} \rho \varsigma^2 (2\partial_x u). \tag{27}$$

With (22), the no-compressibility-error condition (25) is a first-order ordinary differential equation, which admits a unique solution subject to the initial condition $\pi^*(0) = 1/3$,

$$\pi^* = \varsigma^2 [2\sqrt{1 + (u/\varsigma)^2} - 1 - (u/\varsigma)^2]. \tag{28}$$

Direct evaluation verifies that (28) validates the inequalities (20) and is thus asymptotically free; see Figs. 2 and 3. Moreover, it is striking that with the pressure (28), the equilibrium (6) coincides with the entropic equilibrium [21–23]. The latter was postulated in [24] on the basis of the entropy maximum principle and was recently derived also by coarse graining of molecular dynamics [25].

The present derivation highlights the unique renormalizability of the LBM with entropic equilibrium. Note that asymptotically free realizations other than the entropic equilibrium are possible. For example,

$$\pi^* = \varsigma^2 \left[\frac{a(u/\varsigma)^2}{1 + b(u/\varsigma)^2} + 1 - a(u/\varsigma)^2 \right], \tag{29}$$

with $a = 2\varsigma^4/(4\varsigma^2 - 1)$ and $b = \varsigma^4/(a - \varsigma^2)$, also satisfies Eqs. (20), (23), and (24) and is thus linearly stable. Moreover, as can be seen in Fig. 4, the pressure (29) is close in value to the entropic result (28). However, unlike the latter, the pressure (29) still leads to a compressibility error of the same order as the isotropic pressure (8).

C. Sufficient stability condition: Arbitrary lattice Knudsen number

The lattice Knudsen number is defined as $\text{Kn} = (k/2\pi)\delta r$. The above necessary stability condition, derived from the leading-order hydrodynamic limit, pertains to small lattice Knudsen numbers, $\text{Kn} \to 0$. While the necessary stability condition (20) concerns the long-wave limit, the D1Q3 LBGK system allows for analytical study of both the necessary and *sufficient* stability conditions at all wave numbers $k \in [0, 2\pi]$, equivalently at all lattice Knudsen numbers.

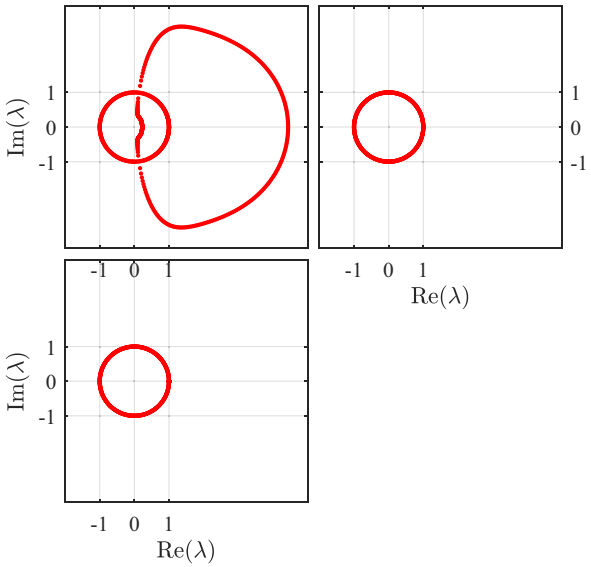

FIG. 5. Root locus of the characteristic polynomial of the D1Q3 LBGK model with $\beta = 0.9994$ and $u = 1$. Top left: Isotropic pressure (8). Top right: Asymptotically free pressure (28). Bottom: Asymptotically free pressure (29).

The necessary and sufficient conditions for linear stability of a discrete system are provided by the concept of Schur stability of the characteristic polynomial [11]. In our case, roots λ of the third-order characteristic polynomial of the linearized LBGK (2) must be located within the unit disk in the complex plane, $|\lambda| \leqslant 1$. To that end, we use a modified Jury table algorithm [26,27] to analytically identify the conditions of Schur stability; details of the analysis can be found in Appendices A and B.

The analysis demonstrates that both the necessary and the sufficient conditions for the linear stability of the D1Q3 LBGK system are *independent* of the wave number. Put differently, the linear stability is independent of the lattice Knudsen number. This proves that the hydrodynamic limit stability condition (20) is both necessary and sufficient for the linear stability of the D1Q3 LBGK.

The effect of the choice of the pressure on the Schur stability is illustrated in Fig. 5: While the isotropic pressure (8) leads to $|\lambda| \geqslant 1$ for some of the roots of the characteristic polynomial and thus to instability, the asymptotically free pressure (28) or (29) guarantees $|\lambda| \leqslant 1$ even for the ultimate velocity value $|u| = 1$.

IV. MULTIDIMENSIONAL SYSTEMS

The above stability condition (20) remains necessary in higher dimensions. Here we consider only the asymptotically free pressure (28). For the LBGK model on the D2Q9 lattice, at the Navier-Stokes order, the nonequilibrium pressure tensor becomes

$$\boldsymbol{\pi}^{\text{neq}} = -\frac{1-\beta}{2\beta} \rho \varsigma^2 [(\boldsymbol{\mathcal{A}} \odot \nabla \boldsymbol{u}) + (\boldsymbol{\mathcal{A}} \odot \nabla \boldsymbol{u})^\dagger], \tag{30}$$

where $\odot$ is the Hadamard (componentwise) product of matrices, while the matrix $\boldsymbol{\mathcal{A}}$ reads

$$\boldsymbol{\mathcal{A}} = \begin{bmatrix} \mathcal{A}_{xx} & \pi^*_{xx}/\varsigma^2 \\ \pi^*_{yy}/\varsigma^2 & \mathcal{A}_{yy} \end{bmatrix}. \tag{31}$$

Here, the off-diagonal components are defined by the pressure (28) as $\pi^*_{\alpha\alpha} = \pi^*(u_\alpha)$, while the diagonal components are defined by the viscosity factor (21) as $\mathcal{A}_{\alpha\alpha} = \mathcal{A}(u_\alpha)$. Thus, with the properties of the function $\mathcal{A}$ already specified, all components of the matrix $\boldsymbol{\mathcal{A}}$ governing the decay rates of both the normal and the shear modes are non-negative in the entire range of flow velocity, $|u_{x,y}| \leqslant 1$. Note that the asymptotics at small velocity, $\boldsymbol{\mathcal{A}} \to \mathbf{1} - \mathrm{diag}\{(2/3)(u_\alpha/\varsigma)^2\}$, where $\mathbf{1}$ is the matrix with all components equal to one, is the same for both the isotropic and the asymptotically free pressure. Together with the linearity of the rate-of-strain $\sim\boldsymbol{\nabla u}$, the remaining anisotropy is of the order of $\sim u^3$ and is a universal consequence of the "cubic anomaly" due to the aforementioned lattice constraint. At the same time, another anomalous term of the order of $\sim u^3$ appears in the nonequilibrium pressure tensor due to compressibility error [proportional to $\mathcal{B}_{\alpha\alpha} = \mathcal{B}(u_\alpha)$; cf. (22)] when the isotropic pressure is used. For the asymptotically free pressure, the latter error is not present in (30), and thus it is more accurate than the isotropic pressure. This is not surprising because the asymptotically free pressure was derived from the no-compressibility-error condition. Moreover, the remaining leading-order anomaly in (31) can be eliminated by renormalization, similar to the D1Q3 case above, albeit within a multiple relaxation time setting rather than the LBGK. This is beyond the scope of this paper.

Schur-stability analysis of the ninth-order characteristic polynomial in two dimensions becomes cumbersome; hence, in the present work, we probe the linear stability of the LBGK by numerically solving the eigenvalue problem. The linear stability domain of the LBGK with the entropic equilibrium of Eq. (28) is compared to the isotropic pressure case in Fig. 6. Also included in the comparison is the second-order polynomial equilibrium [18] obtained by retaining terms of the order of $u_\alpha u_\beta$ in the expansion of the equilibrium populations. It is apparent that LBGK with the asymptotically free equilibrium (28) is unconditionally linearly stable: The stability domain extends to the entire range of flow velocity, $|u| \leqslant 1$, and is independent of the viscosity ν. The two other LBGK with the isotropic pressure behave differently: First, the stability domain is limited by the velocity $|u|^{\max}$ (1), i.e., the value at which isotropic pressure violates the necessary stability condition (20). Above this value, no amount of viscosity can stabilize the LBGK system. Second, the stability domain shrinks to nil with the decrease of the viscosity. All of that is in marked contrast to the asymptotically free LBGK.

V. NUMERICAL SIMULATIONS

A. Sinusoidal density waves

To probe the stability near the $|u| = \pm 1$ limit, simulations were run in a 1D periodic domain of size N_x. The initial

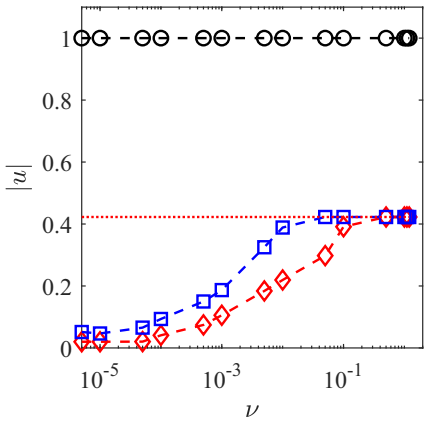

FIG. 6. Linear stability domain of D2Q9 LBGK with different equilibria. Maximal attainable flow velocity vs viscosity (4). Red with diamond markers: Second-order polynomial equilibrium [18]. Blue with square markers: Product-form equilibrium (6) with isotropic pressure (8). Black with circular markers: Product-form equilibrium (6) with asymptotically free pressure (28). Horizontal dotted line: $|u|^{\max} = 1 - 1/\sqrt{3}$ (1).

conditions were

$$\begin{aligned} u(x,0) &= u_0, \\ \rho(x,0) &= \rho_0 + \delta\rho \sin(k_x x), \end{aligned} \tag{32}$$

where $k_x = 2\pi\delta r/N_x$. Velocity u_0 was set very close to its limit, $u_0 = 0.99$, while $\rho_0 = 1$ and $\delta\rho = 10^{-4}$ was set in order to maintain the system in the linear regime, and $N_x = 256$. Simulations were run for different wave numbers, i.e., $k_x \in [0, 2\pi]$, and the energy, $E = \int_x \frac{1}{2}\rho u^2 + \pi^*(\rho - \rho_0)dx$, was monitored over 50 flow-through periods $T = N_x/u_0$. In all simulations, the viscosity was set to $\nu = 10^{-6}$. The total energy evolution in the domain for $k_x = \pi$ is shown in Fig. 7. It is clear from Fig. 7 that the energy in the system stays almost unchanged over this rather long period of time, showing that the system is stable and has low numerical dissipation. For more details on the measured dissipation rate, we refer interested readers to our earlier publication [10]. Similar results are

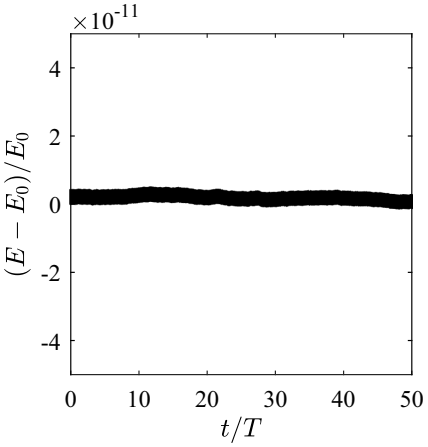

FIG. 7. Evolution of energy in domain for the 1D sinusoidal density waves configuration, for $k_x = \pi$, $u_0 = 0.99$, and $\nu = 10^{-6}$.

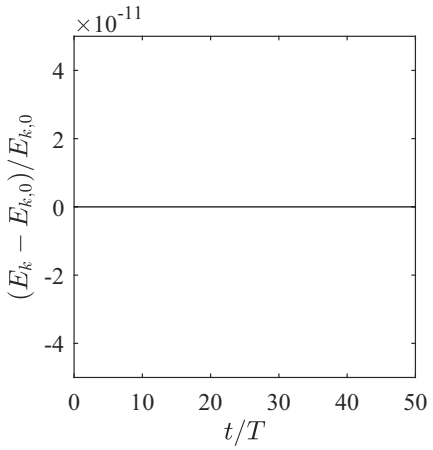

FIG. 8. Evolution of kinetic energy in domain for the 2D shear waves configuration, for $k_x = \pi$, $u_0 = 0.99$, and $\nu = 10^{-6}$.

obtained for all other wave numbers, confirming the analytical results presented in the previous sections.

B. Convected shear modes

To probe the stability of the additional mode brought about in multidimensional cases, we consider a domain of size $N_x \times N_y$ with the following initial conditions:

$$\begin{aligned} u_x(x, y, 0) &= u_0, \\ u_y(x, y, 0) &= \delta u_0 \sin(k_x x), \\ \rho(x, y, 0) &= \rho_0, \end{aligned} \tag{33}$$

where $\rho_0 = 1$ and k_x is defined as for the previous configuration. Here, $\delta u_0 = 10^{-4}$ and $N_x = N_y = 256$. As for the previous configuration, the kinetic energy was proved over 50 flow-through periods for different wave numbers. The viscosity was set to $\nu = 10^{-6}$. The results are illustrated in Fig. 8 for $k_x = \pi$. It is observed that shear modes are stable and have almost vanishing dissipation rates even in the limit of rather large wave numbers, i.e., features resolved by only two grid points.

VI. CONCLUSION

In summary, seminal work on quantum chromodynamics [15,16] teaches us that perturbative computations at low energies in strongly coupled systems are only possible with asymptotic freedom at high energies. Lattice Boltzmann systems can be regarded as strongly coupled in lieu of constraints on the particles' velocities imposed by the lattice; cf. Eq. (10). Thus, stable simulations at low flow velocities may require asymptotic freedom at high velocities.

In order to test this hypothesis, a rigorous approach to the LBM was developed in this paper. The coupling parameter was identified as the equilibrium pressure, while the coarse graining brought about the necessary stability condition, which shows that indeed, the asymptotic freedom must be guaranteed by the equilibrium.

A parallel with the concept of asymptotic freedom can be further demonstrated by looking at the β function [16,17] while identifying π^* as the coupling parameter and u^2 as the energy scale,

$$\beta(\pi^*) = \frac{\partial \pi^*}{\partial \ln(u^2)} = \frac{u}{2}\partial_u \pi^*. \tag{34}$$

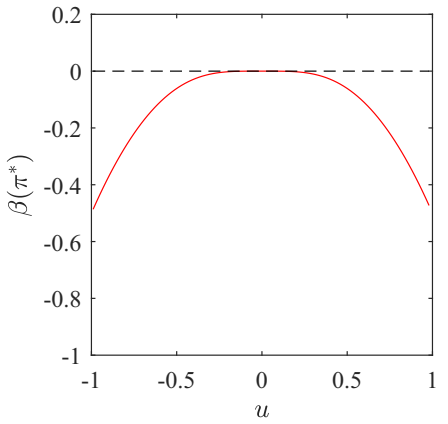

FIG. 9. The β function (34) of the asymptotically free pressure (28).

For the entropic result given by Eq. (28), the β function (34) is plotted in Fig. 9. One clearly observes that for $u \in [-1, 1]$ the β function is nonpositive, $\beta(\pi^*) \leqslant 0$, which agrees with the definition of asymptotic freedom.

It was rigorously shown that the entropic equilibrium satisfies the asymptotic freedom and is uniquely renormalizable. Moreover, for the LBGK model, regularization of the system via asymptotic freedom at vanishing lattice Knudsen number restores linear stability to all lattice Knudsen numbers, that is, the necessary stability conditions are also sufficient. With the asymptotically free equilibrium, the LBGK is unconditionally linearly stable.

Note that while the present work deals with linear stability, the latter is a necessary condition for the overall stability of the LBM. In practice, additional mechanisms will be needed, especially for cases involving strong gradients, for a nonlinear stabilization. This is one argument in favor of one specific form of the asymptotically free LBM: the entropic equilibrium, which comes equipped with an entropy functional and associated nonlinear stabilizer.

The practical outcome of this paper is a rigorous algorithm for the construction of unconditionally linear-stable D1Q3 lattice Boltzmann models based on identification of pressure as the coupling parameter [cf. Eq. (12)], analysis of conditions for asymptotic freedom [cf. Eq. (20)], and solving the resulting renormalization equations [cf. Eq. (25)]. This perspective on the lattice Boltzmann construction may be particularly useful for compressible and multiphase flow LBM simulations [28,29]. A conventional remedy to LBGK instability invokes a concept of multiple relaxation times (MRTs), that is, the relaxation to the equilibrium proceeds at different rates for different moments of the distribution function [3,4]. However, the above analysis shows that the necessary stability condition rather concerns the equilibrium itself. We have performed a numerical stability test on a variety of conventional MRT models to find that all of them are bound to fail when the flow velocity exceeds the same maximum, $|u|^{\max}$ (1) [8]. None of the MRT models with conventional equilibrium produce

unconditionally stable LBM. In an upcoming contribution, through the concept of Schur stability discussed here, reinterpreting MRT schemes as a series of back-to-back relaxation processes between different quasi-equilibria, we will show that the unconditional linear stability of individual quasi-equilibria is necessary for the unconditional linear stability of the scheme in the entire space of the relaxation parameters. In a broader sense, a relation between asymptotic freedom and the entropy maximum principle, which was demonstrated in the above example, may uncover new insights in statistical physics.

ACKNOWLEDGMENTS

This work was supported by European Research Council (ERC) Advanced Grant No. 834763-PonD. Computational resources at the Swiss National Super Computing Center CSCS were provided under Grant No. s1066.

APPENDIX A: SCHUR-STABILITY ANALYSIS

1. Linearization of discrete collision-streaming equation

To perform the linear stability analysis, the collision-streaming evolution equation needs to be linearized as the equilibrium is a nonlinear term. To that end, the discrete distribution function is approximated via a first-order Taylor expansion around $\bar{f}_i$,

$$f_i \approx \bar{f}_i + f_i', \tag{A1}$$

where f_i' is the linear deviation from the reference state. The discrete collision-streaming equation, therefore, changes into

$$f_i'(\boldsymbol{r}+\boldsymbol{c}_i, t+1) = f_i'(\boldsymbol{r}, t) + 2\beta(J_{ij}f_j' - f_i'), \tag{A2}$$

where

$$J_{ij} = \partial_{f_j} f_i^{\mathrm{eq}}\big|_{\bar{f}_j}. \tag{A3}$$

The Jacobian J_{ij} can further be written as

$$J_{ij} = \partial_\rho f_i^{\mathrm{eq}}\big|_{\bar{\rho}} \partial_{f_j}\rho|_{\bar{f}_j} + \partial_{u_\alpha} f_i^{\mathrm{eq}}\big|_{\bar{u}_\alpha} \partial_{f_j} u_\alpha|_{\bar{f}_j}. \tag{A4}$$

Explicit expressions for the Jacobian of the pressure of Eq. (28) can be found in [23]. The solution of the above-linearized discrete system of equations can be written as a combination of monochromatic plane waves,

$$f_i' = F_i' \exp \mathrm{i}(\boldsymbol{k}\cdot\boldsymbol{c}_i - \omega t), \tag{A5}$$

where $F_i' \in \mathbb{C}$, $\|\boldsymbol{k}\| = k$ is the wave number. The physical perturbation can be written as

$$\mathrm{Re}(f_i') = |F_i'| \exp[\mathrm{Im}(\omega)t] \cos[\boldsymbol{k}\cdot\boldsymbol{r} - \mathrm{Re}(\omega)t + \arg(F_i')], \tag{A6}$$

where $\mathrm{Re}(\omega)$ is the real part of ω linked to the wave propagation and $\mathrm{Im}(\omega)$ is the imaginary part tied to its attenuation. Introducing this Fourier expansion in space-time into Eq. (A2) and making use of the notation $\boldsymbol{F}' = [f_1', \ldots, f_Q']^\dagger \in \mathbb{C}^Q$,

$$\exp(\mathrm{i}\omega)\boldsymbol{F} = \mathcal{M}\boldsymbol{F}, \tag{A7}$$

where

$$\mathcal{M}_{ij} = \exp(-\mathrm{i}\boldsymbol{k}\cdot\boldsymbol{c}_i)[2\beta J_{ij} + \delta_{ij}(1-2\beta)]. \tag{A8}$$

2. Characteristic polynomial root locus and positivity

Considering the eigenvalue problem of Eq. (A7), introducing $\lambda = \exp(\mathrm{i}\omega)$, the characteristic polynomial of $\mathcal{M}$ is found as

$$\Lambda(\lambda) = \det(\lambda\boldsymbol{I} - \mathcal{M}). \tag{A9}$$

The linear stability of the corresponding system is guaranteed if and only if $\forall\lambda|\Lambda(\lambda) = 0, \|\lambda\| \leqslant 1$, meaning all roots must be within the unit circle. Such polynomials are called Schur stable [11].

A variety of lemmas have been developed to assess the locus of roots of characteristic polynomials, with real or complex-valued coefficients. Here we use an extension to the Jury table approach [26] proposed in [27]. Considering a characteristic polynomial of degree n,

$$\Lambda(\lambda) = a_n\lambda^n + a_{n-1}\lambda^{n-1} + \cdots + \lambda_0, \tag{A10}$$

with $\forall i \in \{0, \ldots, n\}|a_i \in \mathbb{C}$, the Jury table is defined as follows:

$$\begin{bmatrix} a_n^{(n)} & a_{n-1}^{(n)} & \cdots & a_0^{(n)} \\ a_{n-1}^{(n-1)} & a_{n-2}^{(n-1)} & a_0^{(n-1)} & \\ \cdots & \cdots & & \\ a_1^{(1)} & a_0^{(1)} & & \\ a_0^{(0)} & & & \end{bmatrix},$$

where $a_i^{(n)} = a_i$ and

$$a_{n-i}^{(n-1)} = a_{n-i+1}^{(n)}\bar{a}_n^{(n)} - a_0^{(n)}\bar{a}_{i-1}^{(n)}, \quad i = 1, \ldots, n, \tag{A12a}$$

$$a_{n-i}^{(n-2)} = a_{n-i+1}^{(n-1)}\bar{a}_{n-1}^{(n)} - a_0^{(n-1)}\bar{a}_{i-2}^{(n-1)}, \quad i = 2, \ldots, n, \tag{A12b}$$

$$a_0^{(0)} = \left|a_1^{(1)}\right|^2 - \left|a_0^{(1)}\right|^2. \tag{A12c}$$

Here, the complex conjugate of a variable a is denoted as $\bar{a}$. The polynomial of Eq. (A10) is Schur stable if and only if

$$a_i^{(i)} \geqslant 0 \ \text{ for } i = n-1, \ldots, 0. \tag{A13}$$

APPENDIX B: SCHUR STABILITY OF THE 1D LBGK SYSTEM

1. The D1Q3 lattice: Case of standard pressure

The case of standard pressure corresponds to the case where

$$\pi^* = \varsigma^2 = 1/3, \tag{B1}$$

and leads to a characteristic polynomial of order three,

$$\Lambda(\lambda) = a_3\lambda^3 + a_2\lambda^2 + a_1\lambda + a_0, \tag{B2}$$

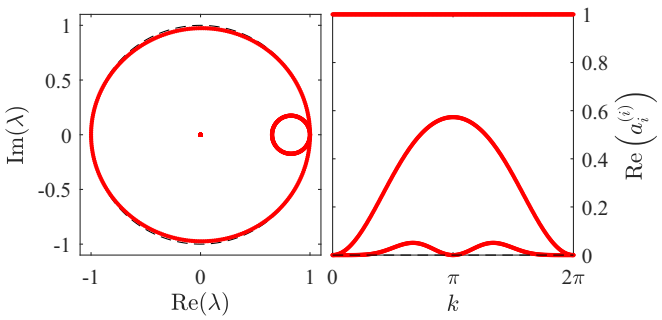

FIG. 10. Root locus (left) and conditions from Jury table (right) for $\beta = 1/2$ and $u = 0.4$ for $\pi^* = \varsigma^2$.

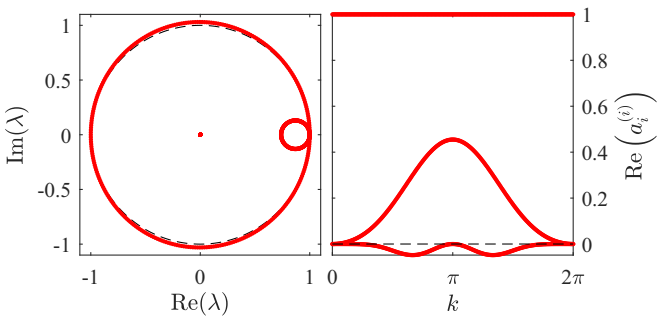

FIG. 11. Root locus (left) and conditions from Jury table (right) for $\beta = 1/2$ and $u = 0.45$ for $\pi^* = \varsigma^2$.

with $a_3 = 1$ and

$$a_2 = [2\beta\varsigma^2 - 2u^2\beta - 2\cos(k) + 2\beta\cos(k) + 2u^2\beta\cos(k) - 2\beta\varsigma^2\cos(k) - 1] + 4u\beta\sin(k)\mathrm{i}, \tag{B3a}$$

$$a_1 = [2\cos(k) - 2\beta - 2u^2\beta + 2\beta\varsigma^2 - 2\beta\cos(k) + 2u^2\beta\cos(k) - 2\beta\varsigma^2\cos(k) + 1] - 4u\beta\sin(k)\mathrm{i}, \tag{B3b}$$

$$a_0 = 2\beta - 1. \tag{B3c}$$

Applying the Jury table algorithm, the following three conditions of stability are recovered:

$$\frac{1}{\beta} - 1 \geqslant 0, \tag{B4a}$$

$$[\cos(k) - 1]u^4 + [2\varsigma^2 - 2\cos(k) - 2\varsigma^2\cos(k) - 4]u^2 + [\cos(k) - \varsigma^4 - 2\varsigma^2\cos(k) + \varsigma^4\cos(k) + 1] \geqslant 0, \tag{B4b}$$

$$u^6 + (3\varsigma^2 + 2)u^4 - (3\varsigma^4 + 1)u^2 + (\varsigma^6 - 2\varsigma^4 + \varsigma^2) \geqslant 0. \tag{B4c}$$

The first condition results in

$$0 < \beta \leqslant 1, \tag{B5}$$

and the second with the third one into

$$|u| \leqslant 1 - \varsigma. \tag{B6}$$

To show the correspondence between the Schur stability and the conditions out of the Jury table, two different cases are illustrated in Fig. 10 and Fig. 11. In the left panels of these figures, the roots of the third-order characteristic polynomial $\Lambda(\lambda)$, given by Eqs. (B2) and (B3a)–(B3c), are shown in the complex plane. In the right panels, the coefficients in the first column of the corresponding Jury table are plotted for different wave numbers k. In Fig. 10, the velocity is taken slightly below the theoretical maximum velocity $u^{\max} = 1 - 1/\sqrt{3}$, and the system is stable as all roots are located within the unit disk in the left panel, while all coefficients of the first column of the Jury table are positive for all wave numbers. This is in contrast to the case of Fig. 11, where the velocity is taken slightly above the theoretical maximum velocity $u^{\max} = 1 - 1/\sqrt{3}$. Then the roots are not always within the unit disk, which leads to negative values in the coefficients of the first column of the Jury table and thus to instability.

2. The D1Q3 lattice: Case of general pressure

In the case of general pressure, the coefficients of the third-order characteristic polynomial are $a_3 = 1$ and

$$a_2 = [2\beta\pi^* - 2\cos(k) - 2u^2\beta + 2\beta\cos(k) - 2\beta\pi^*\cos(k) + 2u^2\beta\cos(k) - 2u\beta\partial_u\pi^* + 2u\beta\partial_u\pi^*\cos(k) - 1] + 2\beta\sin(k)(2u + \partial_u\pi^*)\mathrm{i}, \tag{B7a}$$

$$a_1 = [2\cos(k) - 2\beta + 2\beta\pi^* - 2u^2\beta - 2\beta\cos(k) - 2\beta\pi^*\cos(k) + 2u^2\beta\cos(k) - 2u\beta\partial_u\pi^* + 2u\beta\partial_u\pi^*\cos(k) + 1] - 2\beta\sin(k)(2u + \partial_u\pi^*)\mathrm{i}, \tag{B7b}$$

$$a_0 = 2\beta - 1, \tag{B7c}$$

which lead to the following conditions of stability:

$$\frac{1}{\beta} - 1 \geqslant 0, \tag{B8a}$$

$$[\cos(k) - 1]([\cos(k) - 1]u^4 + 2\partial_u\pi^*[1 - \cos(k)]u^3 + \{2\pi^*[\cos(k) - 1] + \partial_u\pi^{*2}[1 - \cos(k)] + 2[2 + \cos(k)]\}u^2 + 2\partial_u\pi^*\{\pi^*[\cos(k) - 1] + \cos(k) + 2\}u + 2\pi^*\cos(k) + \partial_u\pi^{*2}[1 + \cos(k)] + \pi^{*2}[1 - \cos(k)] - 1 - \cos(k)) \geqslant 0, \tag{B8b}$$

$$[\cos(k) - 1]^3[\cos(k) + 1]\mathcal{Q}(u, \pi^*, \partial_u\pi^*) \geqslant 0, \tag{B8c}$$

where $\mathcal{Q}(u, \pi^*, \partial_u \pi^*)$ is a polynomial of order six in u. Given the sign of the wave-number-dependent coefficients, Eq. (B8c) reduces to the negativity of the polynomial $\mathcal{Q}(u, \pi^*, \partial_u \pi^*)$. Rewriting the polynomial in terms of $\varsigma^{\pm}$ simplifies the expression into the product of two polynomials of order three, $\mathcal{Q}'(u, \varsigma^{\pm})$,

$$\mathcal{Q}'(u, \varsigma^{\pm}) = u^3 + 3\varsigma^{\pm} u^2 + (3\varsigma^{\pm 2} - 1)u + \varsigma^{\pm}(\varsigma^{\pm 2} - 1), \tag{B9}$$

which have the following roots:

$$u_x = \{-(1 + \varsigma^{\pm}),\ \ (1 - \varsigma^{\pm}),\ \ -\varsigma^{\pm}\}, \tag{B10}$$

which correspond exactly to the positive-definiteness condition on total dissipation of Eq. (19). Finally, by simplifying Eq. (B8b), we arrive at the following condition:

$$[1 + \cos(k)](c^{+2} - 1)(c^{-2} - 1) \geqslant 2c^{+}c^{-}(1 + c^{+}c^{-}). \tag{B11}$$

Using the condition obtained from Eq. (B8c), we can readily show that

$$0 \leqslant [1 + \cos(k)](c^{+2} - 1)(c^{-2} - 1) \leqslant 2, \tag{B12}$$

while

$$-2 \leqslant 2c^{+}c^{-}(1 + c^{+}c^{-}) \leqslant 0, \tag{B13}$$

proving that condition (B8c) is automatically satisfied when (B8b) is satisfied. This completes the proof that for a general pressure π^*, the sufficient conditions for stability are the same as the necessary conditions, i.e., positive definiteness of the hydrodynamic dissipation rate.

[1] S. A. Hosseini and I. V. Karlin, Lattice Boltzmann for non-ideal fluids: Fundamentals and practice, Phys. Rep. **1030**, 1 (2023).

[2] S. A. Hosseini, P. Boivin, D. Thevenin, and I. Karlin, Lattice Boltzmann methods for combustion applications, Prog. Energy Combust. Sci. **102**, 101140 (2024).

[3] S. Succi, *The Lattice Boltzmann Equation for Fluid Dynamics and Beyond* (Oxford University Press, Oxford, 2001).

[4] T. Kruger, H. Kusumaatmaja, A. Kuzmin, O. Shardt, G. Silva, and E. M. Viggen, *The Lattice Boltzmann Method: Principles and Practice*, Graduate Texts in Physics (Springer International, Cham, 2017).

[5] R. Benzi, S. Succi, and M. Vergassola, The lattice Boltzmann equation: Theory and applications, Phys. Rep. **222**, 145 (1992).

[6] P. Lallemand and L.-S. Luo, Theory of the lattice Boltzmann method: Acoustic and thermal properties in two and three dimensions, Phys. Rev. E **68**, 036706 (2003).

[7] M. Geier, M. Schönherr, A. Pasquali, and M. Krafczyk, The cumulant lattice Boltzmann equation in three dimensions: Theory and validation, Comput. Math. Appl. **70**, 507 (2015).

[8] S. A. Hosseini, Development of a lattice Boltzmann-based numerical method for the simulation of reacting flows, Ph.D. thesis, Universite Paris-Saclay/Otto-von-Guericke-Universitat Magdeburg, 2020.

[9] P. A. Masset and G. Wissocq, Linear hydrodynamics and stability of the discrete velocity Boltzmann equations, J. Fluid Mech. **897**, A29 (2020).

[10] S. A. Hosseini and I. V. Karlin, Entropic equilibrium for the lattice Boltzmann method: Hydrodynamics and numerical properties, Phys. Rev. E **108**, 025308 (2023).

[11] M. Marden, *Geometry of Polynomials* (American Mathematical Society, Providence, RI, 1949).

[12] M. E. Peskin, *An Introduction to Quantum Field Theory* (CRC Press, Boca Raton, FL, 2018).

[13] J. Zinn-Justin, *Quantum Field Theory and Critical Phenomena*, Vol. 171 (Oxford University Press, Oxford, 2021).

[14] T. Kunihiro, Y. Kikuchi, and K. Tsumura, *Geometrical Formulation of Renormalization-Group Method as an Asymptotic Analysis* (Springer, Singapore, 2022).

[15] D. J. Gross and F. Wilczek, Ultraviolet behavior of non-Abelian gauge theories, Phys. Rev. Lett. **30**, 1343 (1973).

[16] H. D. Politzer, Reliable perturbative results for strong interactions? Phys. Rev. Lett. **30**, 1346 (1973).

[17] D. J. Gross and F. Wilczek, Asymptotically free gauge theories. I, Phys. Rev. D **8**, 3633 (1973).

[18] Y.-H. Qian, D. D'Humières, and P. Lallemand, Lattice BGK models for Navier-Stokes equation, Europhys. Lett. **17**, 479 (1992).

[19] S. Chapman and T. G. Cowling, *The Mathematical Theory of Nonuniform Gases: An Account of the Kinetic Theory of Viscosity, Thermal Conduction and Diffusion in Gases* (Cambridge University Press, Cambridge, 1990).

[20] R. Courant, K. Friedrichs, and H. Lewy, Über die partiellen Differenzengleichungen der mathematischen Physik, Math. Ann. **100**, 32 (1928).

[21] S. Ansumali and I. V. Karlin, Stabilization of the lattice Boltzmann method by the H theorem: A numerical test, Phys. Rev. E **62**, 7999 (2000).

[22] S. Ansumali, I. V. Karlin, and H. C. Öttinger, Minimal entropic kinetic models for hydrodynamics, Europhys. Lett. **63**, 798 (2003).

[23] S. A. Hosseini, M. Atif, S. Ansumali, and I. V. Karlin, Entropic lattice Boltzmann methods: A review, Comput. Fluids **259**, 105884 (2023).

[24] I. V. Karlin, A. Ferrante, and H. C. Öttinger, Perfect entropy functions of the lattice Boltzmann method, Europhys. Lett. **47**, 182 (1999).

[25] T. Blommel and A. J. Wagner, Integer lattice gas with Monte Carlo collision operator recovers the lattice Boltzmann method with Poisson-distributed fluctuations, Phys. Rev. E **97**, 023310 (2018).

[26] E. Jury, Modified stability table for 2D digital filters, IEEE Trans. Circuits Syst. **35**, 116 (1988).

[27] Y. Choo and D. Kim, Schur stability of complex polynomials, J. Inst. Control, Robot. Syst. **15**, 671 (2009).

[28] S. S. Chikatamarla and I. V. Karlin, Entropy and Galilean invariance of lattice Boltzmann theories, Phys. Rev. Lett. **97**, 190601 (2006).

[29] A. Mazloomi M., S. S. Chikatamarla, and I. V. Karlin, Entropic lattice Boltzmann method for multiphase flows, Phys. Rev. Lett. **114**, 174502 (2015).